Electronic Supplementary Information (ESI)

Micro-patterning of C-C covalently-bound grafts by mechanochemical imprint lithography

Xiaoshi Xie,[a] Xiaoli Chang,[a] Shuilong Kang,[a] Yuan Fang*[ac] and Oleksandr Ivasenko*[ab]

[a.] Institute of Functional Nano & Soft Materials (FUNSOM), Soochow University, Suzhou, 215123 Jiangsu, PR China. E-mail: ivasenko@suda.edu.cn, yfang2000@suda.edu.cn
[b.] Jiangsu Key Laboratory of Advanced Negative Carbon Technologies, Soochow University, Suzhou, 215123 Jiangsu, PR China
[c.] Jiangsu Key Laboratory for Carbon-Based Functional Materials & Devices, Soochow University, Suzhou, 215123 Jiangsu, PR China

Content

1. Experimental details

1.1 Covalently functionalized HOPG sample preparation: All covalently functionalized samples were prepared using a custom electrochemical (EC) cell and an electrochemical workstation (CHI660E). A platinum wire electrode served as the counter electrode. The working electrode was Highly Oriented Pyrolytic Graphite (HOPG, ZYB grade) with a typical working area of approximately 0.5 cm^2. The reference electrode used was an Ag/AgCl electrode. An electrolyte was prepared by adding 3,4,5-trimethoxyaniline (2 mM) to 9.8 mL of HCl (50 mM) solution by mixing it with 0.2 mL of $NaNO_2$ (0.1 M). This newly prepared electrolyte was then mixed and shaken for 30 s and immediately introduced into the electrochemical cell. The scan rate was set at 0.05 V/s, covering the redox potentials of aromatic diazonium salts.

1.2 Cleaning of covalently functionalized HOPG samples: At the end of the electrochemical grafting process, the HOPG was disassembled from the electrochemical cell and heated in acetonitrile at 70°C for two hours, and then rinsed thoroughly with ultrapure water (Milli-Q, Millipore, 18.2 MΩ cm), followed by drying under a stream of nitrogen.

1.3 Preparation of PDMS: PDMS precursor and curing agent were mixed at a 10:1 volume ratio. The mixture was degassed using a vacuum pump for 20 minutes to remove any bubbles. The treated PDMS solution was then poured onto the surface of a patterned template and allowed to spread evenly before being heated on a hot plate at 80°C for 30 minutes. After heating, the PDMS was carefully peeled off the template using tweezers.

1.4 MCIL of C-C covalently grafted monolayers using a 2D transfer platform: The patterned PDMS was cut into appropriate sizes and shapes, and adhered to a glass slide using transparent double-sided tape. The slide was then mounted on the movable stage of a high-precision two-dimensional transfer platform (OWTSMP-1), while the functionalized HOPG sample was fixed onto the stage using double-sided tape, ensuring accurate vertical alignment with the PDMS. Subsequently, the height adjustment knob was rotated to bring the PDMS press onto TMP-grafted HOPG for MCIL. Finally, the knob was rotated to separate the PDMS from the HOPG.

1.5 MCIL of C-C covalently grafted monolayers using a semi-automated nanoimprinting set-up: The PDMS with the desired pattern was adhered face up on a glass slide and placed on the stage of a nanoimprint lithography machine (CNI V3.0-100). The HOPG was then gently laid on the surface of the PDMS. Subsequently, the imprint head was closed, and parameters were set (for example, imprint time of 1 minute, with pressures of 1 bar, 2 bar, 3 bar, 4 bar, and 4.5 bar sequentially), before starting the automatic imprinting process. After the imprinting was completed, the imprint head was opened, and HOPG was removed.

1.6 Square/diamond patterns *via* MCIL of C-C covalently grafted monolayers with offset rotation of PDMS stamps: MCIL is conducted on HOPG using a high-precision two-dimensional transfer stage or nanoimprint lithography equipment. Contact between PDMS and HOPG was established either by manually adjusting the height control knob or *via* automatic depression of the imprint head by the apparatus, followed by separation. Subsequently, HOPG was repositioned at a specified angle for another MCIL session, after which HOPG and PDMS were separated again, and the HOPG sample was retrieved.

1.7 Multicomponent patterning: The covalently functionalized HOPG sample (TMP) was first

patterned using a high-precision two-dimensional transfer platform or a nanoimprint lithography machine. Subsequently, TBP (2 mM) was grafted onto the HOPG surface *via* electrochemical grafting. Finally, the sample was washed following the above steps to remove any reaction by-products.

1.8 AFM image analysis: AFM characterization was performed using the Cypher ES (Asylum Research) system at a temperature of 26°C in tapping mode at the air/solid interface. Multi75Al-G probes with a resonance frequency of approximately 75 kHz were used for AFM imaging, producing images with a resolution of 512×512 pixels. In contact mode, the Multi75Al-G probes with a resonance frequency of approximately 40 kHz were used to scan across the functionalized layer. Image analysis was conducted using WSxM 5.0 software[1], with all images subjected to plane fitting and flattening through the application of second-order or higher polynomial fitting.

1.9 STM image analysis: STM image analysis. STM images were obtained using Bruker Multimode V and platinum-iridium wire probe (Pt/Ir). Image analysis was performed using WSxM 5.0 software, and all images were plane-fitted and spread by applying second-order or higher-order polynomial fitting. STM images were acquired according to the constant current mode. The image parameters of the STM images are labelled in the figure notes and denoted by V_{bias} for the sample bias voltage and I_{set} for the tunnelling current.

1.10 SEM image analysis: SEM measurements were conducted using Zeiss G500. The SEM images of the samples were captured at an operating voltage of 10 kV, a probe current of 20 nA, and a working distance of 6.2 mm, the sample was vertically aligned with respect to the secondary-electron emission. The SEM images were utilized to analyse W/P ratios of the patterned samples prepared under different parametric conditions. Uncertainties from multiple measurements within individual SEM images.

1.11 Raman spectroscopic analysis: Raman spectroscopy characterization was conducted using a confocal Raman microscope (Horiba, HR800). The employed laser had a wavelength of 632.8 nm, with the laser beam focused on the sample surface through an objective lens (N.A. = 0.90, working distance 8 mm). The spectrometer was calibrated using a silicon wafer, with an intensity of 10 mW and a spot size of approximately 1 μm. Raman spectra were recorded with a CCD array at -70 °C and the chosen grating had 600 grooves/mm, the accumulation time for each Raman spectrum was 30 seconds. The exact sample movement was provided by an automated xy-scanning table. Raman spectra were acquired from at least five different locations on the sample. All measurements were conducted under ambient room temperature conditions. The I_D/I_G ratio was calculated based on the intensity ratios of the D peak at 1340 cm^{-1} and the G peak at 1580 cm^{-1}, with smoothing and baseline correction performed using Origin software, and results were graphically presented. Raman mapping was per formed based on array scanning in an area of 5 × 5 μm (laser step size in the range of 0.4-0.6 μm, laser energy tuned to 6 mW, integration time set to 1 s).

1.12 Testing reusability of PDMS stamps. Freshly made PDMS stamp with 2μm linear grating was placed on top of clean HOPG and exposed to 1000presses from hand-held commercial vibrating set-up.

---

[1] I. Horcas, R. Fernandez, J.M. Gomez-Rodriguez, J. Colchero, J. Gomez-Herrero and A. M. Baro, Rev. Sci. Instrum., 2007, **78**, 013705

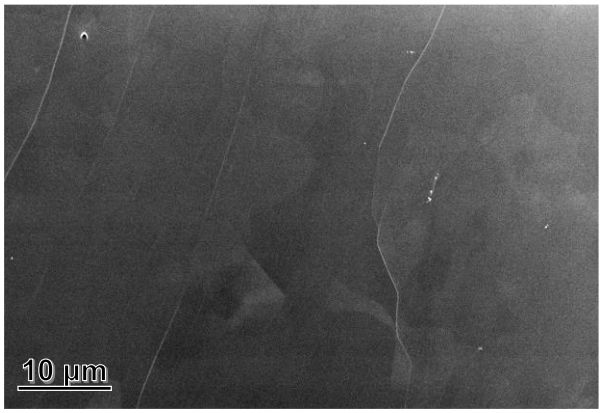

Fig. S1 A representative SEM image of TMP-grafted HOPG surface after an attempted MCIL using a hard polycarbonate grating with a pattern periodicity of 1.5 µm. This image demonstrates the absence of patterned features, underscoring the ineffectiveness of the hard stamp in achieving microscale patterning on the HOPG surface.

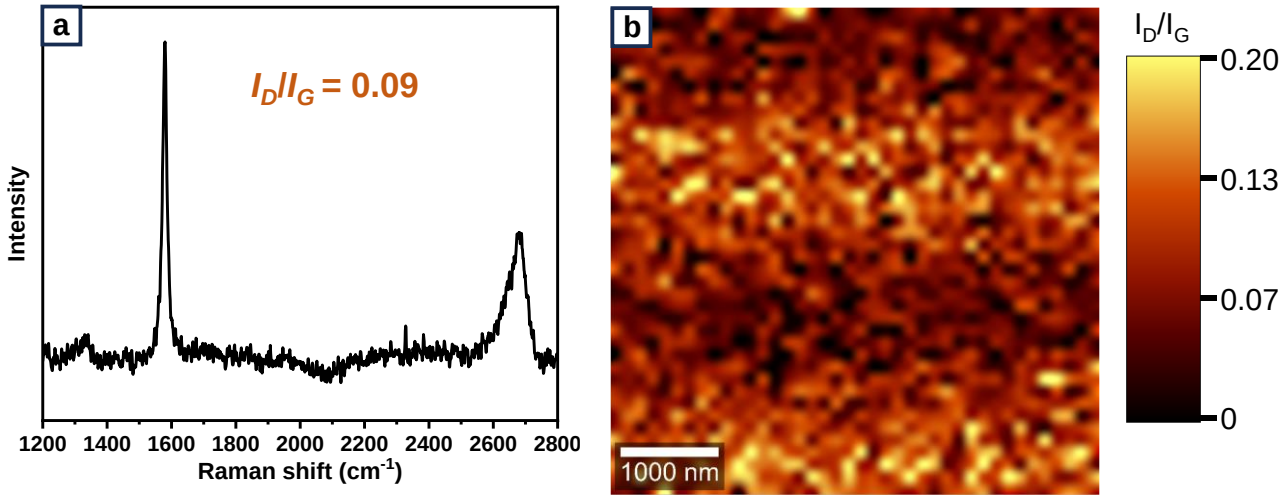

Fig. S2 a) Representative Raman spectra of TMP-grafted HOPG following MCIL with a 2 µm PDMS linear grating. b) Raman map of TMP-grafted HOPG which was MCIL patterned using a 3.3 µm PDMS linear grating.

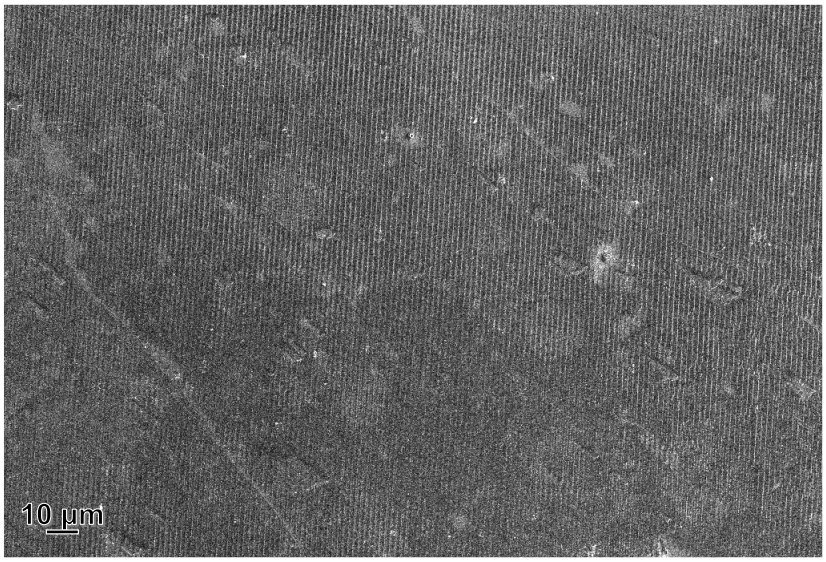

Fig. S3 A representative large-scale SEM image of TMP-grafted HOPG micropatterned by MCIL using 1.5 µm PDMS linear grating.

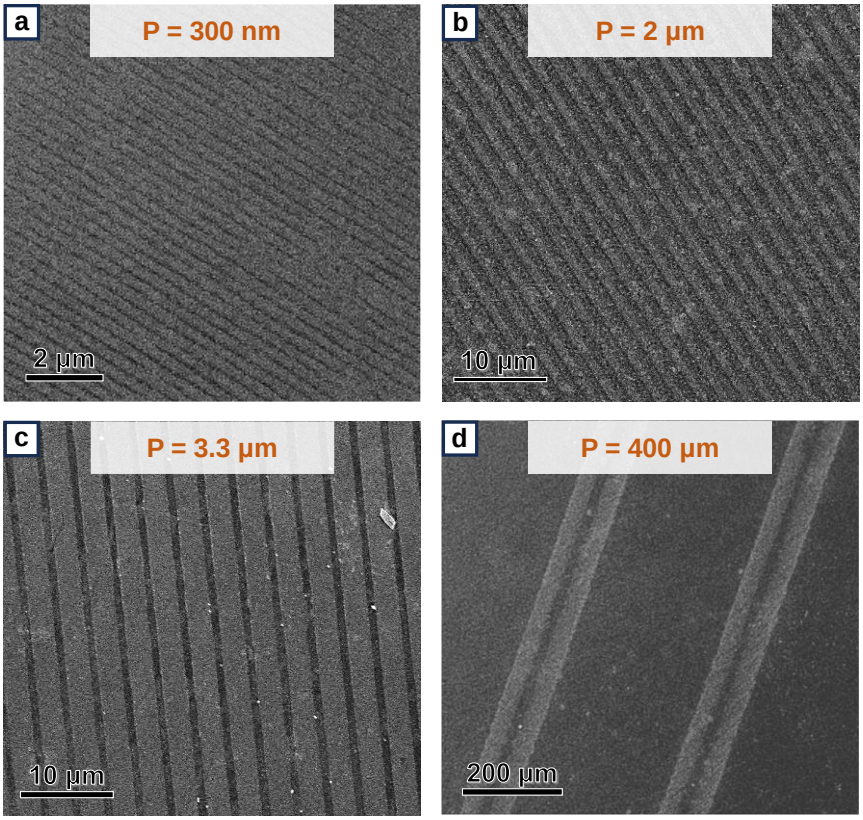

Fig. S4 Representative SEM images of MCIL patterned TMP-HOPG substrates when using linear PDMS gratings with (a) 300 nm, (b) 2.0 µm, (c) 3.3 µm, (d) 400 µm periodicities, respectively.

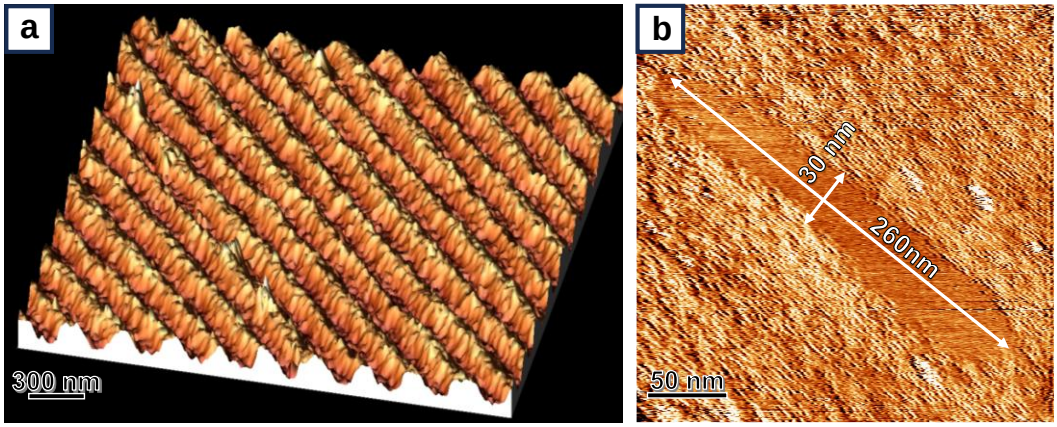

Fig. S5 (a) 3D rendered AFM height image of a 300 nm PDMS linear grating, highlighting the microscale imperfections of the stamp. (b) Scanning tunneling microscopy (STM) image showing defects in TMP-grafted monolayer. Grafting defects are occasionally formed due to surface passivation by physisorbed impurities or nanobubbles. Imaging parameters: I_{set} = 0.04 nA, V_{bias} = -0.8 V.

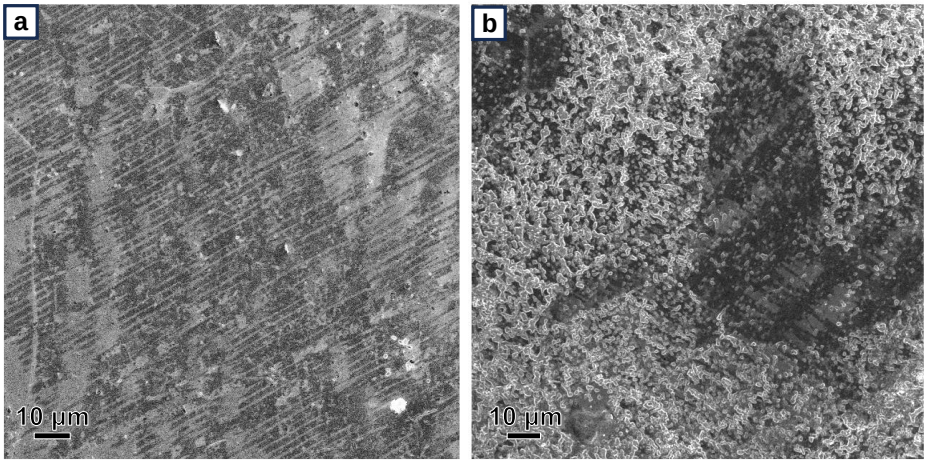

Fig. S6 Initial experiment of MCIL on graphene. MCIL does not pose any special requirement to the substrate, but the quality of the pattern will be greatly affected by the imperfections in the substrate and in the initial grafted layer. Preliminary experiments with different graphene samples have indicated that the primary need for future optimizations lies not with the MCIL but with the functionalization step. Representative SEM images of: (a) a clear MCIL pattern formed on medium quality TMP-grafted graphene samples by using a 2 µm PDMS linear grating; (b) an example of highly defected areas often produced by unoptimized EC-grafting protocol. Probably, such defects are the results of graphene exfoliation and/or copper oxidation during EC grafting.

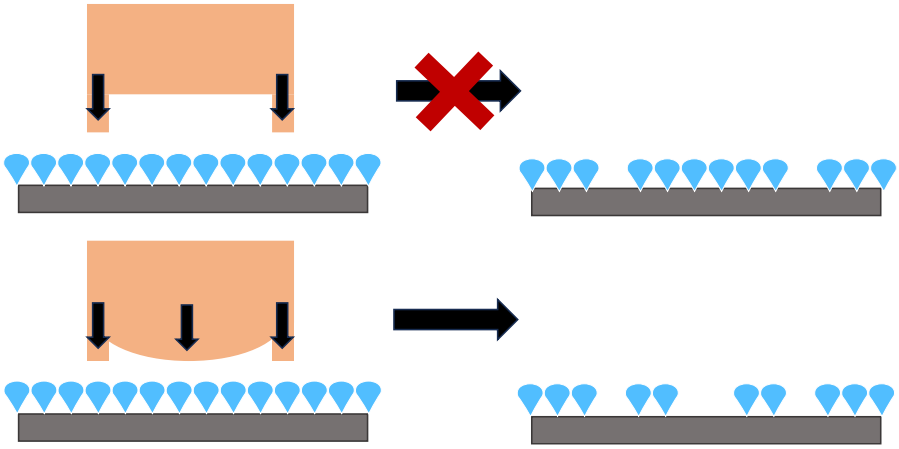

Fig. S7 Schematic illustration explaining the formation of additional degrafted mid-zone due to sagging of PDMS overhang structures.

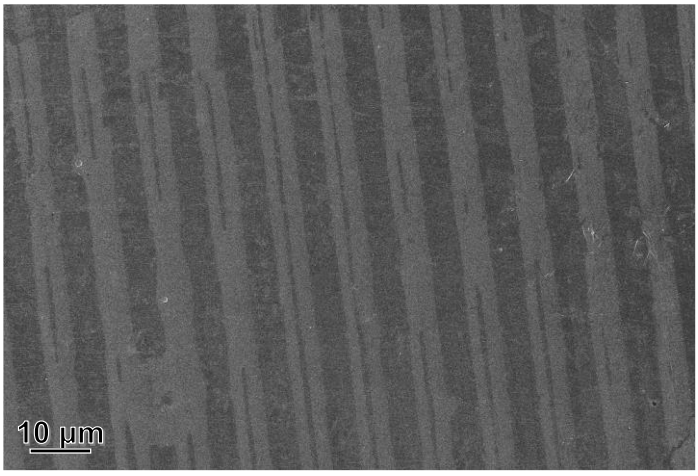

Fig. S8 SEM image of the TMP-grafted HOPG micropatterned by MCIL using 10 µm PDMS linear grating. This image reveals ~1 µm wide degrafting in the central regions of the TMP-grafted stripes, presumably formed due to sagging of PDMS overhang structures during the imprinting process.

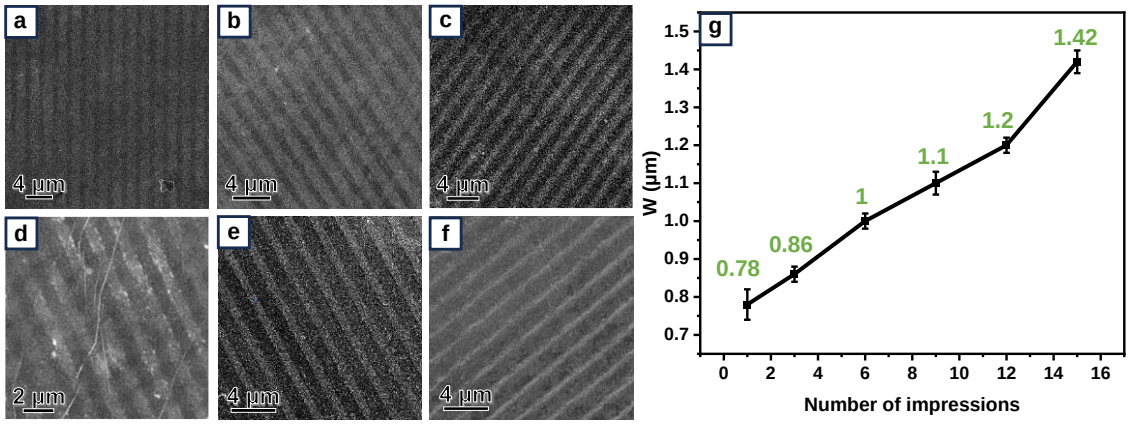

Fig. S9 (a-f) SEM images of TMP-grafted HOPG following multiple MCIL cycles using a PDMS with a pattern periodicity of 2 µm on a high-precision two-dimensional transfer platform. The images show the progression after 1, 3, 6, 9, 12, and 15 cycles, respectively, demonstrating the gradual changes in the microstructure over successive imprinting sessions. (g) Plot illustrating the variation of the degrafting width (W) vs. the number of MCIL cycles, indicating how the pattern dimensions evolve with repeated processing.

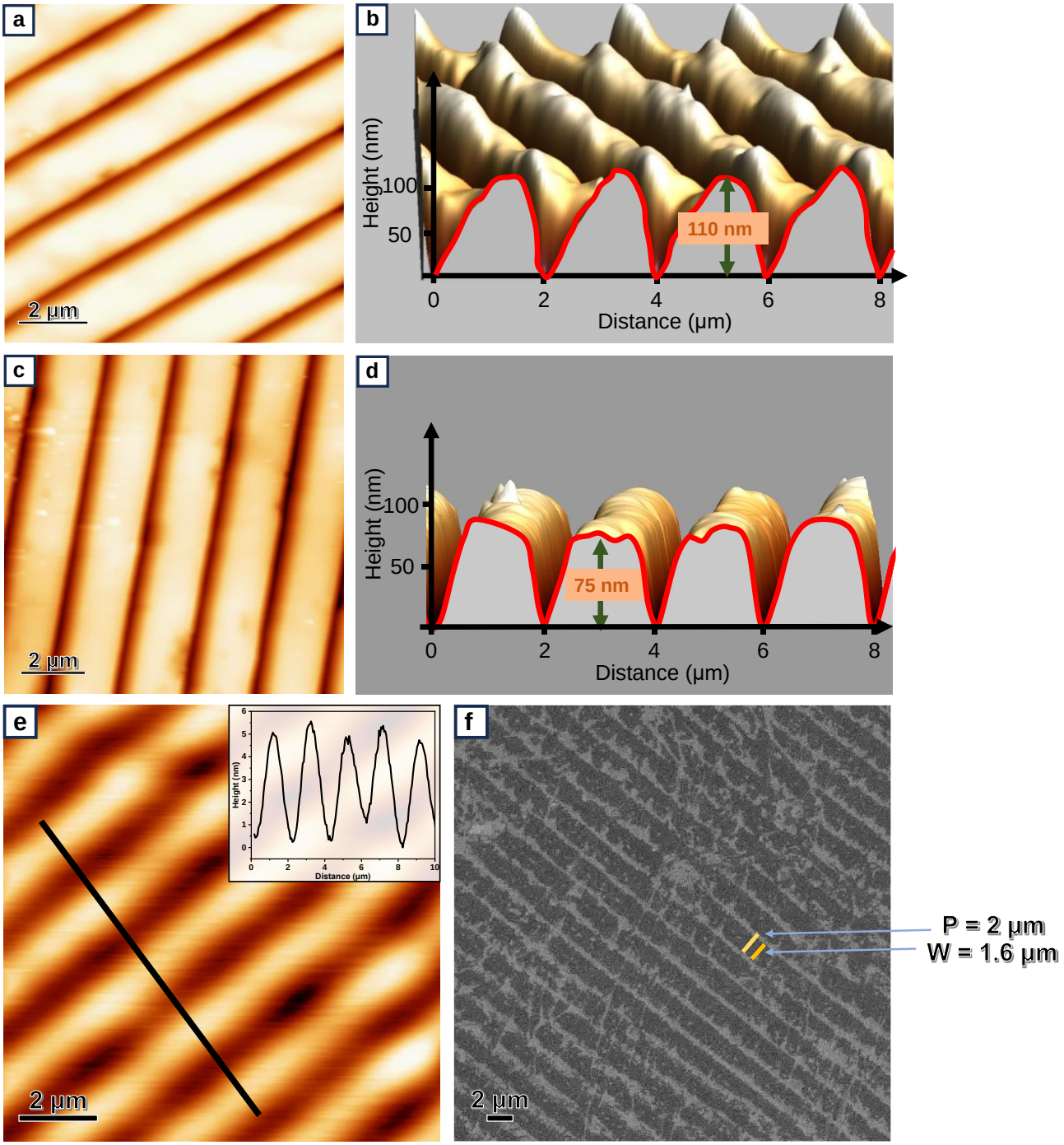

Fig. S10 AFM height images of 2 µm periodic PDMS linear grating before (a), after 3MCIL cycles (c), and after 1000 stamping cycles (e). (b) and (d) show 3D rendering of (a) and (b), respectively. (f) SEM image of TMP-HOPG that was MCIL patterned by the PDMS substrate after 1000 stamping cycles. 3 MCIL cycles (c,d) were performed at a pressure of 4.5 bar, using a nanoimprint lithography machine. PDMS testing in 1000 stamping cycles was done on a home-build set-up without any control of the exact contact pressure. The images highlight the inelastic changes in the topographical features and reduction in peak heights from 110 nm pre-MCIL to 75 nm after 3 MCIL cycles, and to ~5-6 nm after 1000 stamping cycles. Interestingly, despite very shallow depth of the latter PDMS stamp, it can successfully produce 2 µm periodicity linear pattern in TMP-HOPG with degrafting width approaching 1.6 µm.

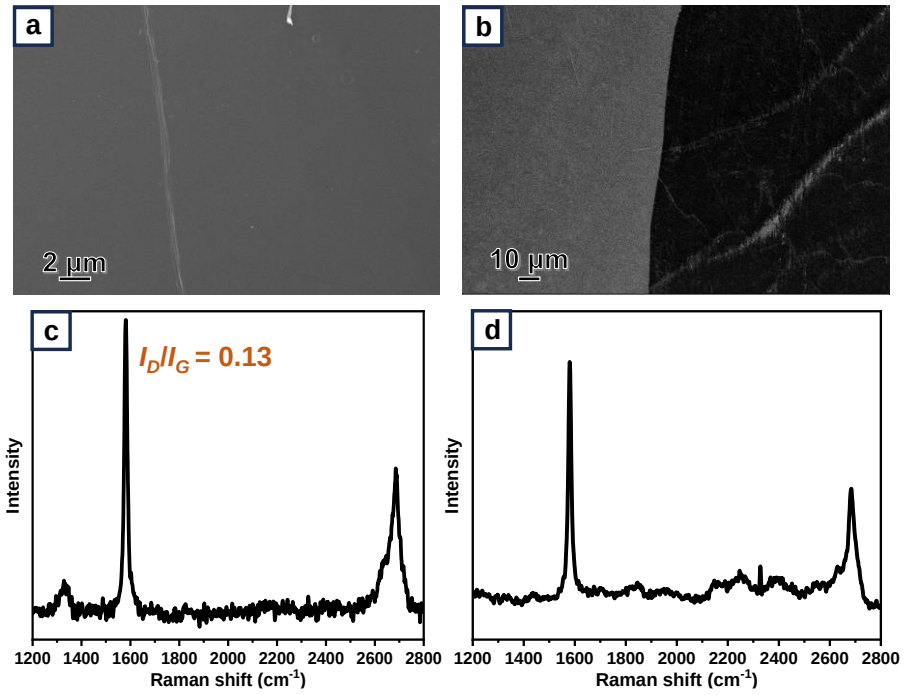

Fig. S11 SEM images and Raman spectrum of TMP-grafted HOPG after full contact with non-patterned flat PDMS stamp applied: (a, c) strictly vertically at 4.5 bar using semi-automatic nanoimprinting set-up; (b, d) vertically till full contact followed by small (<< 1 µm) lateral displacement using the transfer platform. (a) shows unperturbed fully grafted TMP-HOPG as evidenced by high I_D/I_G ratio (c). Left side of (b) is the area that was not touched by PDMS stamp and it is fully grafted, while the right side is completely degrafted as also confirmed by Raman (d).

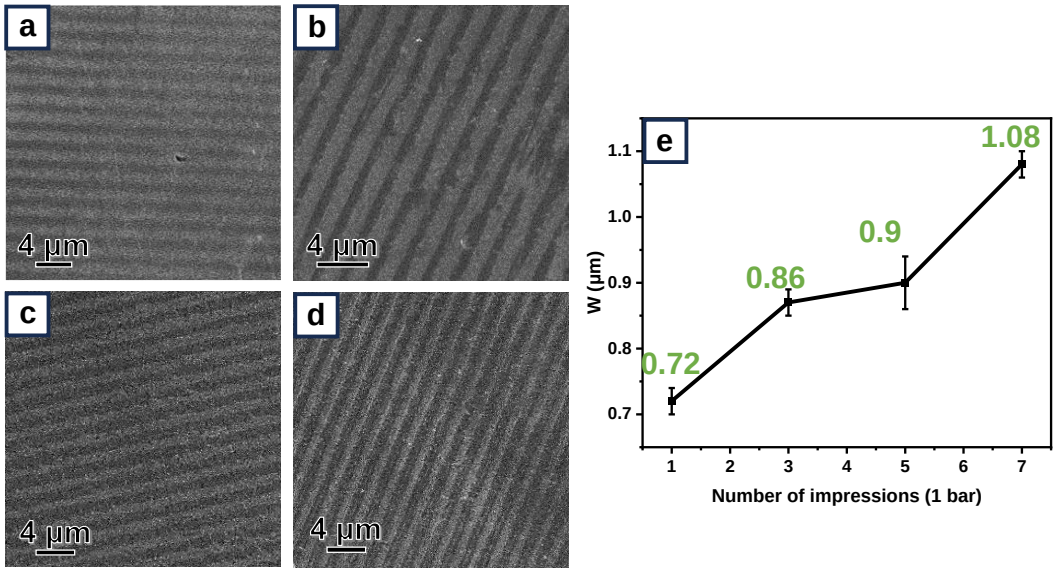

Fig. S12 (a-d) SEM images of TMP-grafted HOPG after 1, 3, 5, and 7 MCIL treatments using a PDMS with a 2 µm pattern periodicity, under a pressure of 1 bar, applied through a nanoimprint lithography machine. (e) Plot of degrafting width (W) *vs.* the number of MCIL cycles, illustrating the progressive changes in pattern dimensions with each additional imprint cycle.

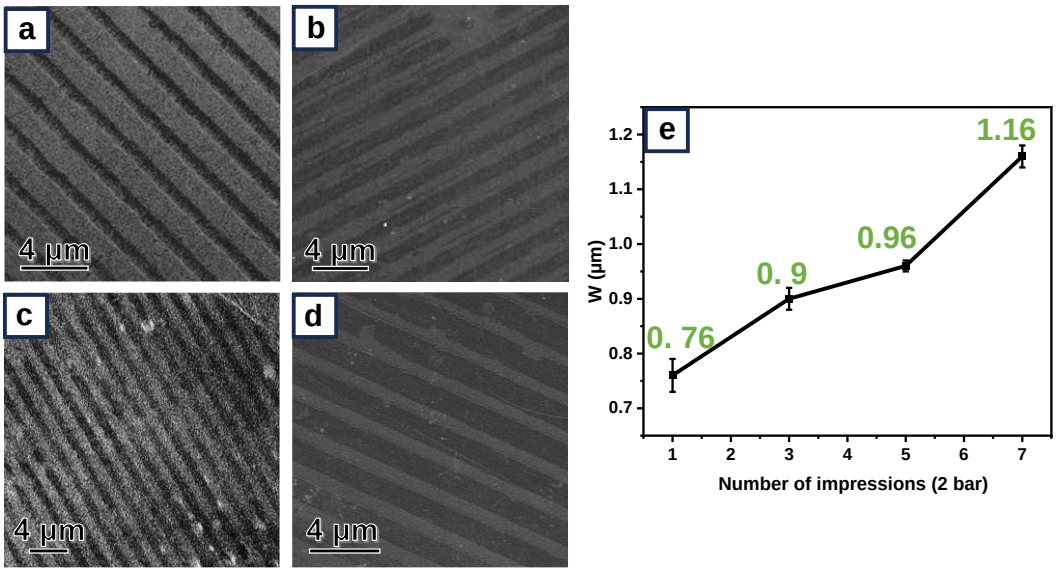

Fig. S13 (a-d) SEM images of TMP-grafted HOPG after 1, 3, 5, and 7 MCIL treatments using a PDMS with a 2 µm pattern periodicity, under a pressure of 2 bar, applied through a nanoimprint lithography machine. (e) Plot of degrafting width (W) *vs.* the number of MCIL cycles, illustrating the progressive changes in pattern dimensions with each additional imprint cycle.

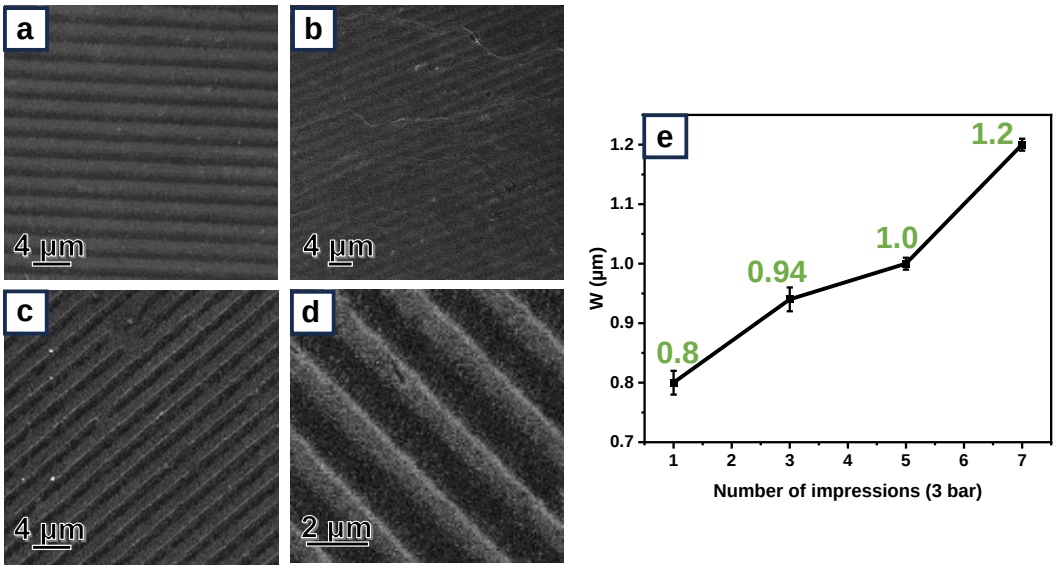

Fig. S14 (a-d) SEM images of TMP-grafted HOPG after 1, 3, 5, and 7 MCIL treatments using a PDMS with a 2 µm pattern periodicity, under a pressure of 3 bar, applied through a nanoimprint lithography machine. (e) Plot of degrafting width (W) *vs.* the number of MCIL cycles, illustrating the progressive changes in pattern dimensions with each additional imprint cycle.

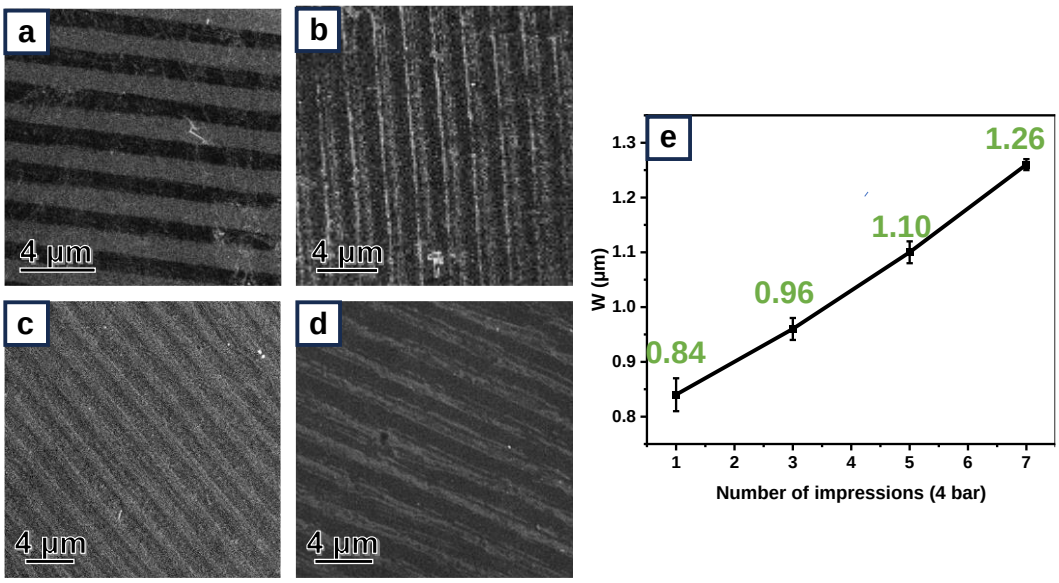

Fig. S15 (a-d) SEM images of TMP-grafted HOPG after 1, 3, 5, and 7 MCIL treatments using a PDMS with a 2 µm pattern periodicity, under a pressure of 4 bar, applied through a nanoimprint lithography machine. (e) Plot of degrafting width (W) vs. the number of MCIL cycles, illustrating the progressive changes in pattern dimensions with each additional imprint cycle.

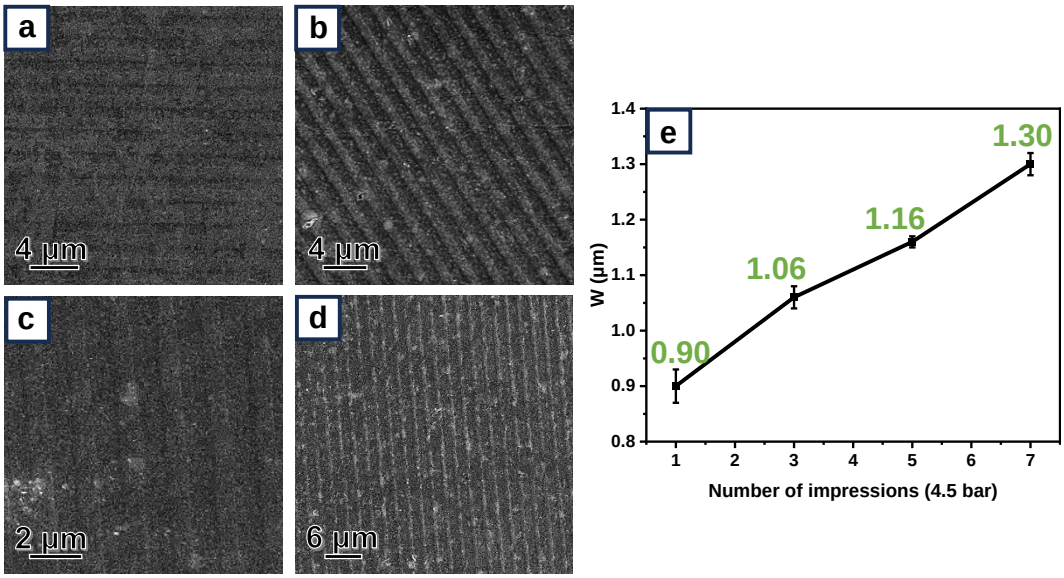

Fig. S16 (a-d) SEM images of TMP-grafted HOPG after 1, 3, 5, and 7 MCIL treatments using a PDMS with a 2 µm pattern periodicity, under a pressure of 4.5 bar, applied through a nanoimprint lithography machine. (e) Plot of degrafting width (W) *vs.* the number of MCIL cycles, illustrating the progressive changes in pattern dimensions with each additional imprint cycle.

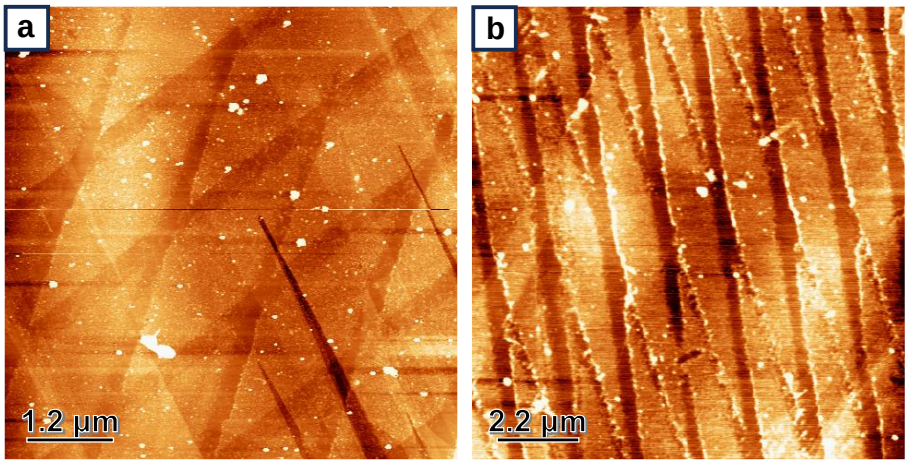

Fig. S17 AFM height images of TMP-grafted HOPG following two consecutive MCIL treatments using a PDMS stamp, which was adjusted for varying pressures and offset angles to create diamond-shaped patterns. These images showcase the diamond patterns with two distinct degrafting widths. This approach highlights the versatile control over pattern dimensions and geometries that can be obtained through careful variations in processing parameters.

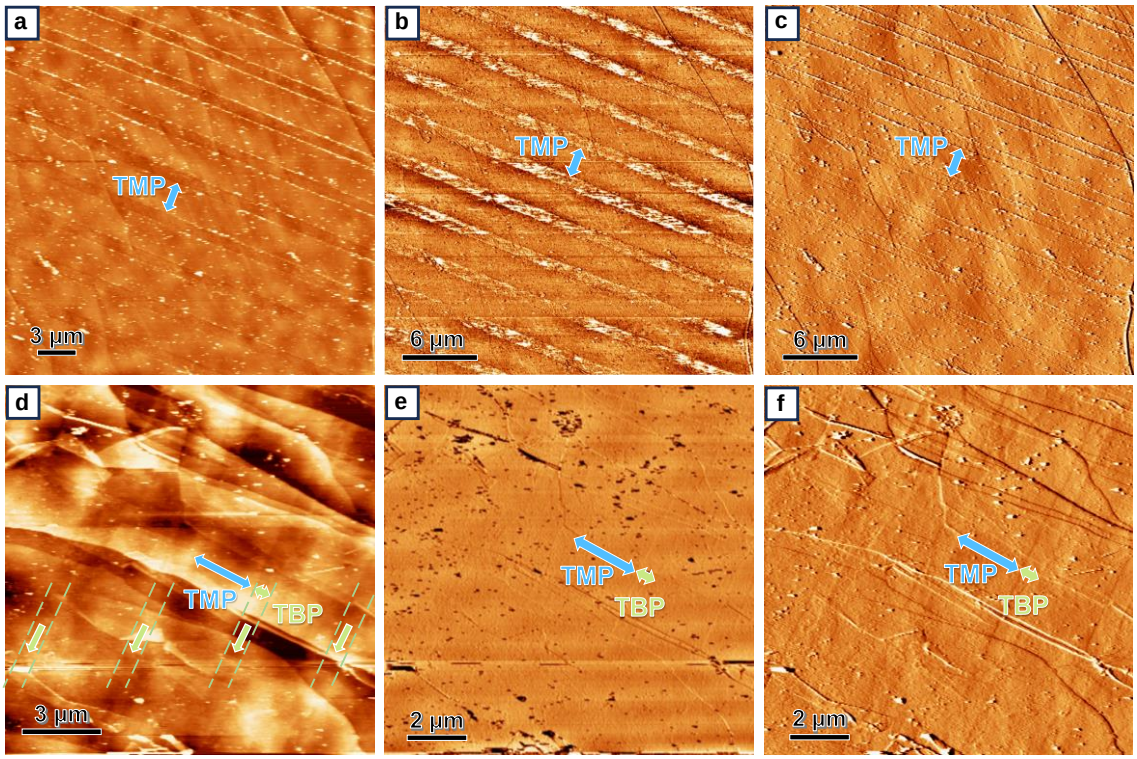

Fig. S18 Multicomponent covalent patterning of HOPG. (a-c) AFM height, phase and amplitude images of the HOPG surface after being grafted with TMP and subjected to MCIL using PDMS stamp with a pattern periodicity of 3.3 µm. (d-f) AFM height, phase and amplitude image of the HOPG surface after covalent patterning with TMP followed by grafting with TBP.

16. Selected answers to specific questions of referees

Question 1.

Reviewer #1: …My main criticism concerns the re-grafting with TBP of areas prepared by local degrafting of TMP monolayers. These experiments are important but not yet convincing. The AFM characterization does not provide convincing evidence of successful re-grafting by TBP. In this respect, the authors admit that the combination of TMP and TBP was not fortunate because their similar size does not provide a height contrast.

We thank the reviewer for this concern and indeed during the revision stage we have successfully done *(please see new Fig. 4 and also see below the answer to the next question*) a much easier-to-distinguish combination for bi-component patterning ($TMP_{(9Å\text{-monolayer})}$-$NBD_{(40Å\text{-dendrimers})}$), but we should point out that:

The originally presented TMP-TBP system is also convincing as the design of the experiment involved **characterization of the films after each step**. Thus, the degrafted grooves in TMP were specifically confirmed to have depth of ~1nm, and were in the sequential TBP grafting completely filled by the ~1nm in full accordance with the expected height of the covalently bound TBP grafts.

Of course thanks to both reviewers' suggestions, the new Fig.4, now showing $TMP_{(9Å\text{-monolayer})}$-$NBD_{(40Å\text{-dendrimers})}$) grafted pattern, is much easier to understand for the readers. The old Fig.4 with TMP-TBP data was moved to SI for completeness.

Question 2

Reviewer #1: …Therefore, for a clear demonstration I would suggest either using two molecules with significantly different lengths, or using some selective chemistry for additional functionalization of one part, or using a chemically sensitive imaging technique.

Reviewer #2: … Is there a reason why molecules of the same height were selected for the multicomponent experiment? Nitro-benzene diazonium could be an option as it is known to lead to dendritic growth

We thank the reviewers for this question. For our future research directions, we are interested in ultrathin monolayers of covalently grafted multi-component patterns that is why the initial choice was focused on TMP and TBP which are known to produce high-quality densely-grafted <1nm thick monolayers. However, we are grateful to both reviewers for their suggestions and fully agree that bi-component pattern in which grafts have clearly different heights helps clarity of the demonstration of the MCIL bi-component patterning. The new Fig. 4 is now showing $TMP_{(9Å\text{-monolayer})}$-$NBD_{(40Å\text{-dendrimers})}$) grafted pattern, which is much easier to understand for the readers. For completeness, the old Fig. 4 with TMP-TBP data was moved to SI.

Question 3

Reviewer #1: ... The relevance of the I_D/I_G ratio as evidence for grafting / degrafting should be briefly explained.

We thank the reviewer for this question. AFM, SEM and Raman together form a convenient and powerful set for the characterization of covalently grafted samples. AFM provides precise measurements of the thickness profile of the patterned grafted layer, and to some extent the micro-/nano-structure of the top surface. SEM

allows large-scale visualization of on-surface micropatterns produced by MCIL. While Raman spectroscopy, and more specifically I_D/I_G ratio provide convenient proof of the covalent nature and semi-quantitative assessment of the surface density of the covalently-bound grafts (e.g. please see the correlation between the diazonium salt concentration, grafting density and I_D/I_G ratio in *ACS Nano*, 2015, **9**, 5520-5535). As a quick example, not grafted HOPG has I_D/I_G of <0.01 (Fig. 1c). This would be the case even if AFM images demonstrate a thick film of physiosorbed impurities. Densely grafted TMP-HOPG that we prepare in this protocol shows I_D/I_G in the range of 0.12-0.2 (e.g. Fig. 1c), but when that sample gets partially degrafted because of successful MCIL micropatterning, the I_D/I_G decreases (e.g. I_D/I_G = 0.09 in 2μm-periodic TMP-HOPG linear pattern in Fig. S2). Ultimately, when one can successfully focus Raman beam and localize patterned area, it is even possible to use I_D/I_G Raman signal for direct visualization of covalently grafted and MCIL-degrafted areas (e.g. the 2D Raman map of TMP-HOPG sample in our new Fig. S2b).

Question 4

Reviewer #1: …Why did the authors use several cycles in Fig. 1b? Please explain.

We thank the reviewer for this question. Electrochemical grafting can be done under different conditions to tune effectively the resulting grafting density as was demonstrated in previous works (e.g. *ACS Nano,* 2019, **13**, 5, 5559–5571; *ACS Nano*, 2015, **9**, 5520-5535). In this project, we simply needed uniform high-density grafting, and as such, any prolonged EC protocol using high concentration (≥2 mM) diazonium salt will work. We choose 100 mV/s cyclic voltammetry protocol and did 3 cycles purely for our own convenience: this allowed us to monitor and qualitatively assess if grafting process proceeded normally. As shown in Fig. 1b, after large electrochemical reduction during the first cycle, the sample is already passivated for further electrochemical response and with each consecutive cycle this passivation increases (not only because the surface is densely grafted but also because insoluble by-products get physiosorbed on the electrode). Furthermore, for us, CV is a convenient way to troubleshoot if there are connection problems (too high / too low current), if diazonium salt has been decomposed or if there are any electrochemically active impurities.

Question 5

Reviewer #1: …Fig. 1b also shows that W becomes larger as the force is increased. This aspect should also be discussed.

We thank the reviewer for this comment. Fig. 1b is CV of grafting, so the reviewer refers here to Fig. 3b in which the degrafting width W is shown to increase as the force increases. Our explanation as well as control experiments (e.g. Fig. S10a-d shows the evidence of inelastic deformation of PDMS after MCIL cycles) were already in the originally submitted text, but to improve readability we have discussed it a bit more. In short: PDMS is an elastic polymer (Poisson's ratio ~0.49, *Soft Matter*, 2019, **15**, 779-784) and with applied force it deforms both elastically and inelastically. Larger compression force widens PDMS microfeatures, leading to the increase of the contact area between PDMS and HOPG, and in turn, this results in a larger number of grafts that got strained and degrafted by PDMS stamp (*i.e.* the degrafted area gets widened).

Question 6

Reviewer #1: ...How many times can a PDMS stamp be used? Is there any evidence of degradation with prolonged use? I would appreciate a brief discussion.

We are grateful to the reviewer for this interesting question. As evidenced from Fig. S9, even after 15 cycles the periodicity of the degrafting pattern is maintained. However, the width of the pattern is changing even if the same pressure is applied (Fig. 3). This is understood to be the result of inelastic deformation of the PDMS stamps (Fig. S10, see also the answer to the previous point), as well as due to the imperfect PDMS-HOPG alignment during consecutive MCIL cycles.

In response to the reviewer's request, we have "overused" freshly made PDMS stamp by attaching it to a vibrating set-up for 1000 stamping cycles. The results are now included in S10e,f. We indeed observe the flattening deformation of the PDMS microfeatures of the stamp: for fixed PDMS grating with 2 μm periodicity, the height of the PDMS grating features drops from ~100-120 nm in the freshly prepared stamps (Fig. S10b) to ~75 nm after 3 MCIL cycles (Fig. S10d) and to ~5-6 nm after 1000 stamping cycles (Fig. S10e). Despite such strong deformation after 1000 stamping cycles, this PDMS stamp successfully created 2 μm patterns on new TMP-HOPG sample, but with the degrafting width now reaching W = 1.6 μm (Fig. S10f).

Finally, we would like to stress that in all our tests we had very limited abilities to simultaneously control stamp-substrate tilt, x-y alignment and pressure. As a result, we often can find regions that were not affected by PDMS stamp. We hope in future to get access to industrial grade equipment which would allow to gain even better fine-tuning of the MCIL protocols.